Journal of Crystal Growth 131 (1993) 607–611
North-Holland

Growth of MgTe and $Cd_{1-x}Mg_xTe$ thin films by molecular beam epitaxy

A. Waag, H. Heinke, S. Scholl, C.R. Becker and G. Landwehr
Physikalisches Institut, Universität Würzburg, Am Hubland, D-97074 Würzburg, Germany

Received 26 March 1993; manuscript received in final form 22 April 1993

We report on the growth of the compound semiconductor MgTe as well as the ternary alloy $Cd_{1-x}Mg_xTe$ by molecular beam epitaxy. This is to our knowledge the first time that this material has been grown by any epitaxial technique. Bulk MgTe, which is hygroscopic, has a band gap of 3.0 eV and crystallizes usually in the wurtzite structure. Pseudomorphic films were grown on zincblende CdTe substrates for a MgTe thickness below a critical layer thickness of approximately 500 nm. In addition, $Cd_{1-x}Mg_xTe$ epilayers were grown with a Mg concentration between 0 and 68%, which corresponds to a band gap between 1.5 and 2.5 eV at room temperature. The crystalline quality of the layers is comparable to CdTe thin films as long as they are fully strained. The lattice constant of zincblende MgTe is slightly smaller than that of CdTe, and the lattice mismatch is as low as 0.7%. In addition highly n-type CdMgTe layers were fabricated by bromine doping. The tunability of the band gap as well as the rather good lattice match with CdTe makes the material interesting for optoelectronic device applications for the entire visible range.

1. Introduction

II–VI semiconductors are interesting candidates for future optoelectronic devices. On the one hand II–VI compounds containing Hg cover the whole infrared spectrum, whereas the wide gap II–VI semiconductors offer direct band gaps through the entire visible range to the ultraviolet. Recently, the first blue light emitting semiconductor laser diode was fabricated on the basis of ZnSe [1]. CdTe exhibits many interesting features: a band gap in the middle of the solar spectrum, a high atomic weight for X-ray detection, and an electro-optic coefficient, which is about a factor of 4 higher than in GaAs [2]. In addition, CdTe is the base material for the related ternary alloys $Hg_{1-x}Cd_xTe$ and $Cd_{1-x}Mn_xTe$ (CdMnTe). $Hg_{1-x}Cd_xTe$ is an important infrared detector material, and CdMnTe as a dilute magnetic semiconductor exhibits unique features such as, e.g., a giant Faraday rotation and magnetic polaron formation [3,4].

In principle, CdMnTe is a potential material for light emitting devices covering the whole visible range: MnTe is a wide gap semiconductor with a band gap of 3.2 eV, and recently an electron injected CdMnTe/CdTe quantum well laser emitting in the red range of the visible spectrum was fabricated [5]. On the other hand, the lattice mismatch to CdTe is relatively high (2.3%), leading to a small critical layer thickness or a high dislocation density. This is especially relevant for higher manganese concentrations. Therefore we have searched for an alternative material with a better lattice matching to CdTe, which in a ternary alloy with CdTe would cover the entire visible region.

The bulk properties of MgTe as well as those of the ternary alloys $Cd_{1-x}Mg_xTe$ and $Zn_{1-x}Mg_xTe$ have been studied by different groups [6–15]. MgTe is hygroscopic, and the surface is very rapidly oxidized under standard environmental conditions. Chemical reaction with water produces MgO and H_2Te. H_2Te decomposes immediately at room temperature, and the tellurium produces a black residue [10]. Therefore the properties of pure MgTe are hard to ascertain. However, the ternary alloys $Cd_{1-x}Mg_xTe$ are sta-

0022-0248/93/$06.00 © 1993 – Elsevier Science Publishers B.V. All rights reserved

ble if the magnesium content does not exceed a certain critical value. For $Cd_{1-x}Mg_xTe$, the critical Mg content is not known. In the past, bulk crystals have been fabricated with Mg contents of up to 60% without the above-mentioned chemical reaction [12]. $Cd_{1-x}Mg_xTe$ with Mg content above 60% has been found to crystallize in the wurtzite structure and between 30% and 65% various polytypes were obtained [12].

In the following we report on the growth and characterization of MgTe and $Cd_{1-x}Mg_xTe$ thin films by molecular beam epitaxy (MBE). This is to our knowledge the first time that $Cd_{1-x}Mg_xTe$ was grown by any epitaxial technique. $Cd_{1-x}Mg_xTe$ layers were grown with Mg concentrations between 0 and 0.68. The binary compound MgTe was grown by using elemental Te and Mg sources. The thin films have been characterized by reflection high energy electron diffraction (RHEED), X-ray diffraction, optical reflection as well as transport measurements.

2. Experimental procedure

Thin films were grown on (001) oriented CdTe substrates. The substrates were chemomechanically polished using a bromine–methanol–ethyleneglycol solution. Before insertion into the MBE system, the substrates were etched with HCl and subsequently rinsed in deionized water. A heat treatment in vacuum at 350°C for 15 min in the presence of a Cd flux was used to clean the substrate surface. Before the growth of the $Cd_{1-x}Mg_xTe$ layers, a CdTe buffer of 200 nm thickness was grown at a substrate temperature of 315°C. The $Cd_{1-x}Mg_xTe$ layers themselves were grown at a substrate temperature of 250°C. A CdTe compound source as well as an elemental Mg source were used for the $Cd_{1-x}Mg_xTe$ MBE growth, whereas elemental Mg and Te sources were used for the growth of the binary compound MgTe. The growth temperatures of the Mg cell were in the range between 200 and 300°C. The Mg beam equivalent pressures (Mg BEPs) were measured using an ion gauge at the substrate position.

RHEED was used to monitor the growth in

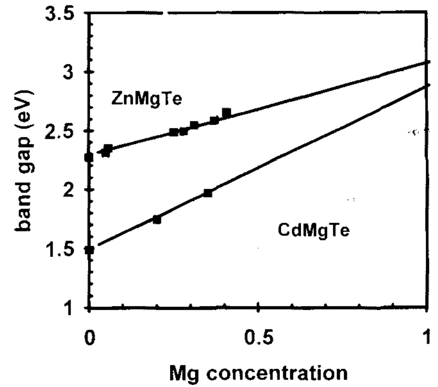

Fig. 1. Band gap of $Cd_{1-x}Mg_xTe$ and ZnMgTe as a function of Mg content [8,13]. Only data for the zincblende material are included. To determine the x-value of our $Cd_{1-x}Mg_xTe$ thin films, the band gap was measured via optical reflection and subsequently the calibration curve for $Cd_{1-x}Mg_xTe$ was used.

situ. The band gap was determined by room temperature reflection measurements using a Bruker Fourier transform spectrometer (IFS 88). The lattice constants as well as the structural quality of the layers were determined using a five/six crystal X-ray diffractometer. Free electron concentration as well as carrier mobility of n-doped $Cd_{1-x}Mg_xTe$ layers were determined by making use of the Van der Pauw method using a Drude model for data analysis. For this, a magnetic field of 0.3 T was employed, and indium contacts were fabricated by thermobonding.

Fig. 1 shows band gap values of $Cd_{1-x}Mg_xTe$ and ZnMgTe taken from the literature for different Mg x-values [8,13]. Only data from ternary alloys with cubic structure have been included. From this, a band gap for the cubic semiconductor MgTe between 2.9 and 3. 1 eV is derived from a linear extrapolation. To determine the x value of our thin films of zincblende $Cd_{1-x}Mg_xTe$ grown by MBE, the calibration curve in fig. 1 for bulk cubic $Cd_{1-x}Mg_xTe$ was used and the band gap was determined experimentally.

3. Results and discussion

At the substrate temperature used (250°C), pronounced RHEED oscillations could be ob-

served after the growth start of MgTe on the CdTe buffer. This shows that the growth regime of MgTe is compatible with the one of CdTe. During the first ≅ 100 nm of MgTe growth, the RHEED diffraction pattern showed a streaky (2 × 1) reconstruction. At larger thicknesses, the RHEED pattern became more and more spotty, and beyond 500 nm a relatively abrupt change from cubic symmetry to a more or less polycrystalline pattern occurred. We believe that the MgTe layer then grew in the wurtzite structure, which was found to be the stable crystal structure in MgTe bulk material.

MgTe is known to be very reactive at room atmosphere. Therefore we have tried to protect the MgTe surface with a CdTe cap of varying thickness. After deposition of approximately 400 nm MgTe, when the RHEED pattern started to look spotty but nevertheless was still cubic, a CdTe cap was grown at the same substrate temperature. During the growth of the CdTe film, the quality of the RHEED pattern improved, and finally the pattern showed streaks again. However, neither a 100 nm nor a 1000 nm thick CdTe cap could prevent the MgTe from being oxidized at room atmosphere. Therefore no additional investigations have been done on MgTe thin films. For the 1000 nm CdTe cap, the oxidation took longer, but nevertheless the MgTe surface was oxidized after approximately 30 min. The reason why the thick CdTe cap could not protect the MgTe surface is unclear at the moment.

The band gaps of the $Cd_{1-x}Mg_xTe$ thin films were determined by means of room temperature optical reflection measurements. In fig. 2 the reflection at room temperature in the energy range between 0.15 and 2.6 eV is shown for 2 layers with different x-values. The band gap of the CdTe substrate as well as the band gap of the $Cd_{1-x}Mg_xTe$ thin films can clearly be identified in spite of the interference patterns, and they are indicated in the figure. From this, the x-value of the thin films was derived using fig. 1. In our case, the band gap corresponds to x-values of 0.33% and 0.68%. The $Cd_{1-x}Mg_xTe$ layers were chemically stable at environmental conditions. No oxidation of the thin films could be observed.

One should also mention the very large amplitudes of the interference fringes, which reflect a large difference in the index of refraction between the CdTe substrate and the $Cd_{1-x}Mg_xTe$ thin films. The high frequency dielectric constant of bulk MgTe has been found to be 3.7 [12], in contrast to 7.2 for CdTe and 5.9 for ZnSe [16].

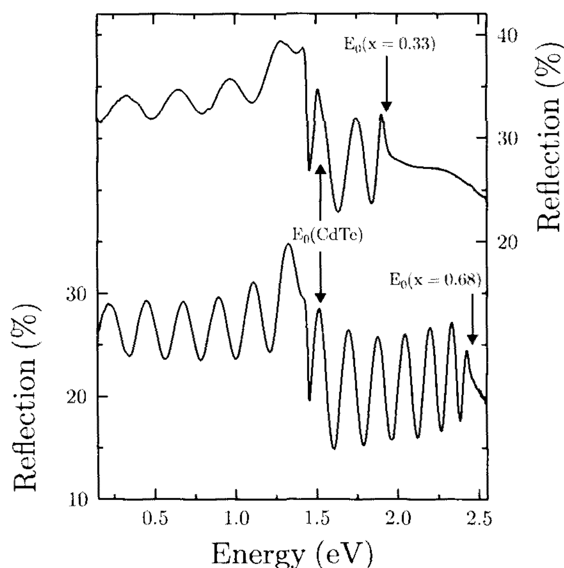

Fig. 2. Optical reflection at room temperature for $Cd_{1-x}Mg_xTe$ thin films on CdTe substrate for two different x-values. The Mg x-value was derived from the $Cd_{1-x}Mg_xTe$ band gap (arrows).

To check the lattice constant as well as the structural quality of the $Cd_{1-x}Mg_xTe$ layers, X-ray diffraction measurements have been performed. The strain in the layers has been investigated by reciprocal space mapping of asymmetric reflections. From this a strain parameter γ was deduced, which reflects the degree of relaxation of the layers: $\gamma = 1$ corresponds to a fully strained layer, whereas $\gamma = 0$ describes a fully relaxed layer. The strain parameter γ is given by

$$(a_{\text{layer}} - a_{\text{sub}})_{\text{parallel}}/a_{\text{sub}} = (1-\gamma)(a_{\text{layer}} - a_{\text{sub}})_{\text{relaxed}}/a_{\text{sub}}.$$

A tilt between substrate and layer orientation has been measured by reciprocal space mapping of the symmetric (004) reflection and taken into account in the strain analysis described above.

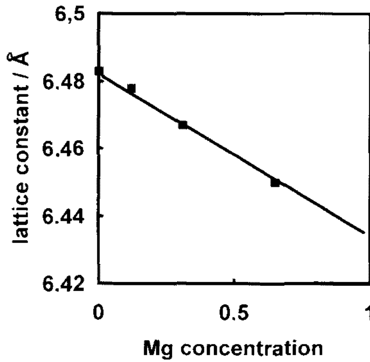

Fig. 3. $Cd_{1-x}Mg_xTe$ lattice constant as a function of Mg concentration. A lattice constant for the zincblende MgTe of 6.435 Å is derived, which corresponds to a lattice mismatch of only 0.7% to CdTe.

The Poisson number of MgTe used in this analysis was assumed to be equal to that of CdTe.

All $Cd_{1-x}Mg_xTe$ layers investigated by X-ray diffraction were found to have a zincblende symmetry (layer thickness: 800 nm). The zincblende lattice constant of MgTe as extrapolated from lower x-values was found to be 6.435 ± 0.002 Å, which corresponds to a lattice mismatch of 0.7% to CdTe and 0.5% to CdZnTe (3.5% Zn). The unstrained lattice constants of undoped $Cd_{1-x}Mg_xTe$, the strain in the layers as well as the rocking curve width of the (004) reflex are summarized in table 1. For higher Mg contents, the rocking curve widths are larger, corresponding to a higher degree of strain relaxation and therefore a larger number of misfit dislocations in the layers.

Table 1
X-ray diffraction results for $Cd_{1-x}Mg_xTe$ thin films; FWHM(004) is the full width at half maximum of rocking curves using the (004) reflex and γ is the strain parameter of the layers; $\gamma = 1$ corresponds to a layer fully strained to the lateral lattice constant of the CdTe substrate and $\gamma = 0$ corresponds to a fully relaxed thin film; the lattice constant is that for the unstrained zincblende lattice

Sample	x(Mg)	FWHM(004) (arcsec)	γ	Lattice constant (Å)
CT626	0.12	72	0.87	6.478
CT627	0.33	250	0.52	6.467
CT619	0.68	450	0.28	6.450

Table 2
Results of bromine doping of $Cd_{1-x}Mg_xTe$ thin films for various Mg concentrations. n is the reciprocal Hall number at room temperature and μ is the electron Hall mobility at room temperature, both derived from Van der Pauw measurements; for higher Mg content, a steep decrease in dopant activation is found, similiar to the halogen doping of CdMnTe; for comparison: the resisitivity of undoped layers usually is above 10^3 Ω cm

Sample	x(Mg)	n (cm^{-3})	μ ($cm^2/V\cdot s$)	Resistivity (Ω cm)
CT628	0.10	8×10^{17}	453	1.7×10^{-2}
CT629	0.30	3×10^{15}	100	1.5×10^{1}
CT631	0.65	Not measurable	–	–

Recently, Zn-halogen compounds have been successfully used for the n-type doping of CdTe and CdMnTe, resulting in resistivities of 5×10^{-3} Ω cm for both CdTe and CdMnTe [17,18]. To test the doping possibilities of $Cd_{1-x}Mg_xTe$, we have used $ZnBr_2$ as an n-type dopant. The free carrier concentration as well as the carrier mobility have been determined by Hall effect measurements making use of the Van der Pauw method.

In the doping experiments growth parameters such as substrate temperature and all fluxes were kept constant with the exception of the Mg flux, which was varied from sample to sample. In pure CdTe, the $ZnBr_2$ flux used in these experiments leads to a doping level of approximately 1×10^{18} cm^{-3}. The results of the $Cd_{1-x}Mg_xTe$ doping attempts are summarized in table 2, where the free carrier concentration, Hall mobility and re-

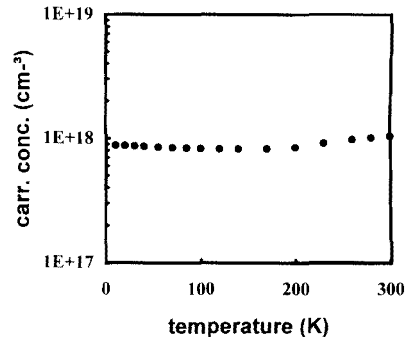

Fig. 4. Free carrier concentration of a bromine doped n-type $Cd_{1-x}Mg_xTe$ thin film ($x_{Mg} = 0.10$) as a function of temperature.

sisitivity are shown for samples with different Mg contents. A result of these preliminary experiments is that doping is efficient for low Mg content, whereas it drastically deteriorates at higher Mg content (33% and above). A similiar behavior has been observed in CdMnTe [18]. The reduction in mobility also reflects the decreasing structural quality of the films. Again it is not clear at this stage whether this behavior is merely due to an increasing number of dislocations in the films with higher Mg content. Further investigations are needed to clarify this point.

Fig. 4 shows the temperature dependence of the free carrier concentration between 300 and 4 K for doped $Cd_{1-x}Mg_xTe$ layer with 10% Mg. The free carrier concentration remains constant as expected for a degenerately doped sample.

4. Summary

We have demonstrated the feasibility of growing cubic MgTe as well as $Cd_{1-x}Mg_xTe$ by molecular beam epitaxy. To our knowledge this is the first time that $Cd_{1-x}Mg_xTe$ layers have been grown by any epitaxial technique. $Cd_{1-x}Mg_xTe$ can serve as a new barrier material for CdTe based quantum well structures. The small lattice mismatch to CdTe (0.7%) is advantagous compared to CdZnTe and CdMnTe. In addition CdMgTe can be used for non-magnetic barriers in $Cd_{1-x}Mg_xTe$/CdMnTe dilute magnetic quantum well structures with magnetic CdMnTe quantum wells. The band gap of $Cd_{1-x}Mg_xTe$ can be tuned through the whole visible region of the spectrum, making the material interesting for optoelectronic applications. Further work has to be done to test the doping limits of $Cd_{1-x}Mg_xTe$, especially for $Cd_{1-x}Mg_xTe$ with a band gap in the visible.

Acknowledgements

We want to thank M. Bruder (AEG Heilbronn) for supplying us with CdTe source material, as well as P. Wolf for the substrate preparation. This project was supported by the Bundesminister für Forschung und Technologie, Bonn.

References

[1] M. Haase, J. Qiu, J. DePuydt and H. Cheng, Appl. Phys. Letters 59 (1991) 1272.
[2] J. Pankove, Optical Processes in Semiconductors (Dover, New York, 1971) p. 346.
[3] J.K. Furdyna, J. Appl. Phys. 64 (1988) R29.
[4] D.R. Yakovlev, W. Ossau, G. Landwehr, R.N. Bicknell-Tassius, A. Waag S. Schmeusser, I.N. Uraltsev, A. Pohlmann and E.O. Göbel, J. Crystal Growth 117 (1992) 854.
[5] J. Cibert, C. Bodin-Deshayes, G. Feuillet, P.H. Joneau, Le Si Dang and E. Molva, Mater. Sci. Eng. B 16 (1993) 279.
[6] G.A. Saum and E. Hensley, Phys. Rev. 113 (1959) 1019.
[7] R. Yamamoto, M. Inoue, K. Itoh and T. Shitaya, Japan. J. Appl. Phys. 6 (1967) 537.
[8] R. Yamamoto and K. Itoh, Japan. J. Appl. Phys. 8 (1969) 341.
[9] S.G. Parker, A.R. Reinberg, J.E. Pinnell and W.C. Holton, J. Electrochem. Soc. Solid State Sci. 118 (1971) 979.
[10] A. Kuhn, A. Chevy and M.-J. Naud, J. Crystal Growth 9 (1971) 263.
[11] S. Nakashima, T. Fukumoto, A. Mitsuishi and K. Itoh, J. Phys. Soc. Japan 32 (1972) 1438.
[12] S. Nakashima, T. Fukumoto, A. Mitsuishi and K. Itoh, J. Phys. Soc. Japan 35 (1973) 1437.
[13] D. Barbier and A. Laugier, Solid State Commun. 23 (1977) 435.
[14] D. Boulanger and M.-S. Martin, Phys. Status Solidi (b) 85 (1978) 597.
[15] B. Montegu, A. Laugier and D. Barbier, Phys. Rev. B 19 (1979) 1920.
[16] D.T.F. Marple, J. Appl. Phys. 35 (1964) 539.
[17] D. Hommel, A. Waag, S. Scholl and G. Landwehr, Appl. Phys. Letters 61 (1992) 546.
[18] A. Waag, S. Scholl, K. von Schierstedt, D. Hommel, G. Landwehr and G. Bilger, J. Crystal Growth 129 (1993) 243.